

# Combination therapy with hydrogen peroxide and irradiation promotes an abscopal effect in mouse models

Naoya Kemmotsu<sup>1,2</sup> | Li Zhu<sup>1,3</sup> | Joji Nagasaki<sup>1</sup> | Yoshihiro Otani<sup>2</sup> | Youki Ueda<sup>1</sup> | Hiromichi Dansako<sup>1</sup> | Yue Fang<sup>3</sup>  | Isao Date<sup>2</sup> | Yosuke Togashi<sup>1</sup> 

<sup>1</sup>Department of Tumor Microenvironment, Graduate School of Medicine, Dentistry and Pharmaceutical Sciences, Okayama University, Okayama, Japan

<sup>2</sup>Department of Neurological Surgery, Graduate School of Medicine, Dentistry and Pharmaceutical Sciences, Okayama University, Okayama, Japan

<sup>3</sup>Department of Microbial and Biochemical Pharmacy, School of Pharmacy, China Medical University, Shenyang, Liaoning, China

## Correspondence

Yosuke Togashi, Department of Tumor Microenvironment, Okayama University Graduate School of Medicine, Dentistry and Pharmaceutical Sciences, 2-5-1 Shikata-cho, Kita-ku, Okayama 700-8558, Japan.

Email: [yogashi1584@gmail.com](mailto:yogashi1584@gmail.com)

## Funding information

KORTUC Inc, Grant/Award Number: N/A

## Abstract

Hydrogen peroxide (H<sub>2</sub>O<sub>2</sub>) induces oxidative stress and cytotoxicity, and can be used for treating cancers in combination with radiotherapy. A product comprising H<sub>2</sub>O<sub>2</sub> and sodium hyaluronate has been developed as a radiosensitizer. However, the effects of H<sub>2</sub>O<sub>2</sub> on antitumor immunity remain unclear. To investigate the effects of H<sub>2</sub>O<sub>2</sub>, especially the abscopal effect when combined with radiotherapy (RT), we implanted murine tumor cells simultaneously in two locations in mouse models: the hind limb and back. H<sub>2</sub>O<sub>2</sub> mixed with sodium hyaluronate was injected intratumorally, followed by irradiation only at the hind limb lesion. No treatment was administered to the back lesion. The H<sub>2</sub>O<sub>2</sub>/RT combination significantly reduced tumor growth at the noninjected/nonirradiated site in the back lesion, whereas H<sub>2</sub>O<sub>2</sub> or RT individually did not reduce tumor growth. Flow cytometric analyses of the tumor-draining lymph nodes in the injected/irradiated areas showed that the number of dendritic cells increased significantly with maturation in the H<sub>2</sub>O<sub>2</sub>/RT combination group. In addition, analyses of tumor-infiltrating lymphocytes showed that the number of CD8<sup>+</sup> (cluster of differentiation 8) T cells and the frequency of IFN-γ<sup>+</sup> (interferon gamma) CD8<sup>+</sup> T cells were higher in the noninjected/nonirradiated tumors in the H<sub>2</sub>O<sub>2</sub>/RT group compared to those in the other groups. PD-1 (programmed death receptor 1) blockade further increased the antitumor effect against noninjected/nonirradiated tumors in the H<sub>2</sub>O<sub>2</sub>/RT group. Intratumoral injection of H<sub>2</sub>O<sub>2</sub> combined with RT therefore induces an abscopal effect by activating antitumor immunity, which can be further enhanced by PD-1 blockade. These findings promote the development of H<sub>2</sub>O<sub>2</sub>/RT therapy combined with cancer immunotherapies, even for advanced cancers.

## KEYWORDS

abscopal effect, dendritic cell, hydrogen peroxide, radiosensitizer, radiotherapy, tumor-draining lymph node

**Abbreviations:** CD, cluster of differentiation; DAMPs, damage-associated molecular patterns; DCs, dendritic cells; ER, endoplasmic reticulum; H<sub>2</sub>O<sub>2</sub>, hydrogen peroxide; IFN-γ, interferon gamma; mAb, monoclonal antibody; PD-1, programmed death receptor 1; RT, radiotherapy; SCID, severe combined immunodeficiency; TDLNs, tumor-draining lymph nodes.

Naoya Kemmotsu and Li Zhu contributed equally to this work.

This is an open access article under the terms of the [Creative Commons Attribution-NonCommercial](https://creativecommons.org/licenses/by-nc/4.0/) License, which permits use, distribution and reproduction in any medium, provided the original work is properly cited and is not used for commercial purposes.

© 2023 The Authors. *Cancer Science* published by John Wiley & Sons Australia, Ltd on behalf of Japanese Cancer Association.

## 1 | INTRODUCTION

Radiotherapy (RT) plays an important role in the treatment of cancer, along with surgery and anticancer drugs, and is currently used for a variety of purposes, including curative and palliative therapy.<sup>1,2</sup> However, radioresistance occurs at times; this is partially caused by the presence of hypoxic cells and antioxidant enzymes, such as peroxide and catalase, that neutralize the reactive oxygen species generated by RT.<sup>3</sup> To overcome this, hydrogen peroxide (H<sub>2</sub>O<sub>2</sub>) mixed with sodium hyaluronate (KRC-01 or KORTUC®) was developed as a radiosensitizer.<sup>4</sup> When H<sub>2</sub>O<sub>2</sub> is injected into the tumor, antioxidant enzymes, such as peroxidase and catalase, are deactivated. Simultaneously, oxygen molecules are produced from the decomposition of H<sub>2</sub>O<sub>2</sub>; this can improve hypoxic conditions in tumors.<sup>5</sup> Clinical trials for breast (NCT03946202) and cervical cancer (NCT05570422) have been conducted.<sup>6,7</sup>

The concept of the abscopal effect was first introduced by Mole in 1953, and it refers to the regression of metastatic tumors located far from the irradiated field.<sup>8</sup> Since then, abscopal effects have been reported in breast cancer,<sup>9</sup> melanoma,<sup>10,11</sup> hepatocellular carcinoma,<sup>12</sup> renal cell carcinoma,<sup>13</sup> and non-small-cell lung cancer.<sup>14,15</sup> The mechanism of this abscopal effect in response to radiation is not fully understood; however, the prevailing hypothesis is that the effect is primarily due to the activation of antitumor immunity.<sup>16</sup> Irradiated tumors release damage-associated molecular patterns (DAMPs), which activate the immune system, leading to an abscopal effect.<sup>16</sup> However, the abscopal effect of H<sub>2</sub>O<sub>2</sub> with RT has not been evaluated. Here, we investigated the abscopal effects and mechanisms underlying the combination therapy using intratumoral H<sub>2</sub>O<sub>2</sub> injection and RT in mouse models. In addition, we evaluated the efficacy of the combination therapy with PD-1 blockade using the same model.

## 2 | MATERIALS AND METHODS

### 2.1 | Cell lines and reagents

The MC-38 cell line (murine colon cancer) was obtained from Kerastat. The B16F10 cell line (murine melanoma) was obtained from the American Type Culture Collection. These cell lines were maintained in DMEM (FUJIFILM Wako Pure Chemical Corporation) supplemented with 10% fetal bovine serum (FBS; Thermo Fisher Science). All tumor cells were used after confirming that they were *Mycoplasma* (-) using the PCR Mycoplasma Detection Kit (TaKaRa), according to the manufacturer's instructions. The rat anti-mouse PD-1 monoclonal antibody (mAb) (RMP1-14) and control rat IgG2a mAb (RTK2758) were obtained from BioLegend.

### 2.2 | In vitro HMGB1 and calreticulin assay

MC-38 cells (1 × 10<sup>5</sup>) were treated with H<sub>2</sub>O<sub>2</sub> (10 μM or 50 μM), RT (5 Gy), or a combination of both. Twenty-four hours later, the

supernatants and cells were collected for HMGB1 and calreticulin assays, respectively. HMGB1 levels were measured by ELISA using an HMGB1 detection kit (Promega) according to the manufacturer's instructions. For calreticulin, we evaluated its expression on the cell surface using flow cytometry.

### 2.3 | In vivo animal models

Female C57BL/6J mice (6–8 weeks old) were purchased from SLC Japan. C57BL/6J-Prkdc<sup>scid</sup>/Rbrc mice (B6 SCID; RBRC01346) were obtained from RIKEN BRC. Cells were inoculated subcutaneously into the left hind limb (MC38:1 × 10<sup>6</sup>, B16F10:5 × 10<sup>5</sup>) and right back (MC38:5 × 10<sup>5</sup>, B16F10:2.5 × 10<sup>5</sup>). Tumor volume was monitored every 3 days. The means of the long and short diameters were used to generate tumor growth curves. Tumors and iliac lymph nodes (tumor-draining lymph nodes [TDLNs]) were harvested 14 days after tumor cell inoculation for evaluation using flow cytometry. All in vivo experiments were performed at least twice. All the mice were maintained under specific pathogen-free conditions at the animal facility of the Institute of Biophysics. Animal experiments were approved by the Animal Committee for Animal Experimentation of Okayama University. All experiments met the US Public Health Service Policy on Human Care and Use of Laboratory Animals.

### 2.4 | In vivo treatment

When tumor volume in the left hind limb reached approximately 100 mm<sup>3</sup> (before day 10), 0.25 mL of 0.5% w/v H<sub>2</sub>O<sub>2</sub> (Oxydol; Ken-ei Pharmaceutical) mixed with 0.83% w/v sodium hyaluronate (Meiji Seika Pharma) was immediately administered directly into the center of the tumors at one site in the left hind limb. Within 30 min after dosing, 15-Gy single dose irradiation was applied to the same tumors using MBR-1520R-3 (15 mA with a 0.5 mm Al and 0.2 mm Cu filter; Hitachi) at a rate of approximately 1 Gy/min. During irradiation, a custom fixation device was used to prevent irradiation of tumors on the back (Figure S1). Anti-PD-1 mAb (200 μg/mouse) or control mAb was administered intraperitoneally three times every 3 days after H<sub>2</sub>O<sub>2</sub> injection and irradiation on day 10.

### 2.5 | Flow cytometry analyses

Flow cytometry assays were performed as previously described.<sup>17,18</sup> Briefly, the cells were washed with PBS containing 2% FBS and stained with surface antibodies. The samples were assessed using FACS Fortessa (BD Biosciences) and FlowJo software (BD Biosciences). Staining antibodies were diluted according to the manufacturer's instructions. For intracellular cytokine staining, a protein transport inhibitor (BD Biosciences) was added for the last 4 h of culture with phorbol myristate acetate (PMA; Selleck) and ionomycin

(Cayman Chemical). The antibodies used in the flow cytometry analyses are summarized in Table S1.

## 2.6 | Statistical analysis

GraphPad Prism 8 (GraphPad Software) was used for statistical analyses. The relationships among groups were compared using one-way analysis of variance (ANOVA). The relationships between tumor volume curves were compared using two-way ANOVA. For multiple testing, Bonferroni corrections were employed. All tests were two-tailed and  $P$  values  $<0.05$  were considered statistically significant.

## 3 | RESULTS

### 3.1 | The $H_2O_2$ /RT combination treatment induces an abscopal effect

First, we examined whether  $H_2O_2$ /RT combination treatment induced an abscopal effect in mouse models, using MC38 and B16F10 cell lines (Figure 1A). In clinical settings,  $H_2O_2$  mixed with hyaluronate is injected into multiple sites on large tumors.<sup>7</sup> However, in our mouse models, the tumors were so small that the mixture would spread over the entire tumor after injecting at one site, therefore we injected at only one site in the center of the tumors. Tumor growth

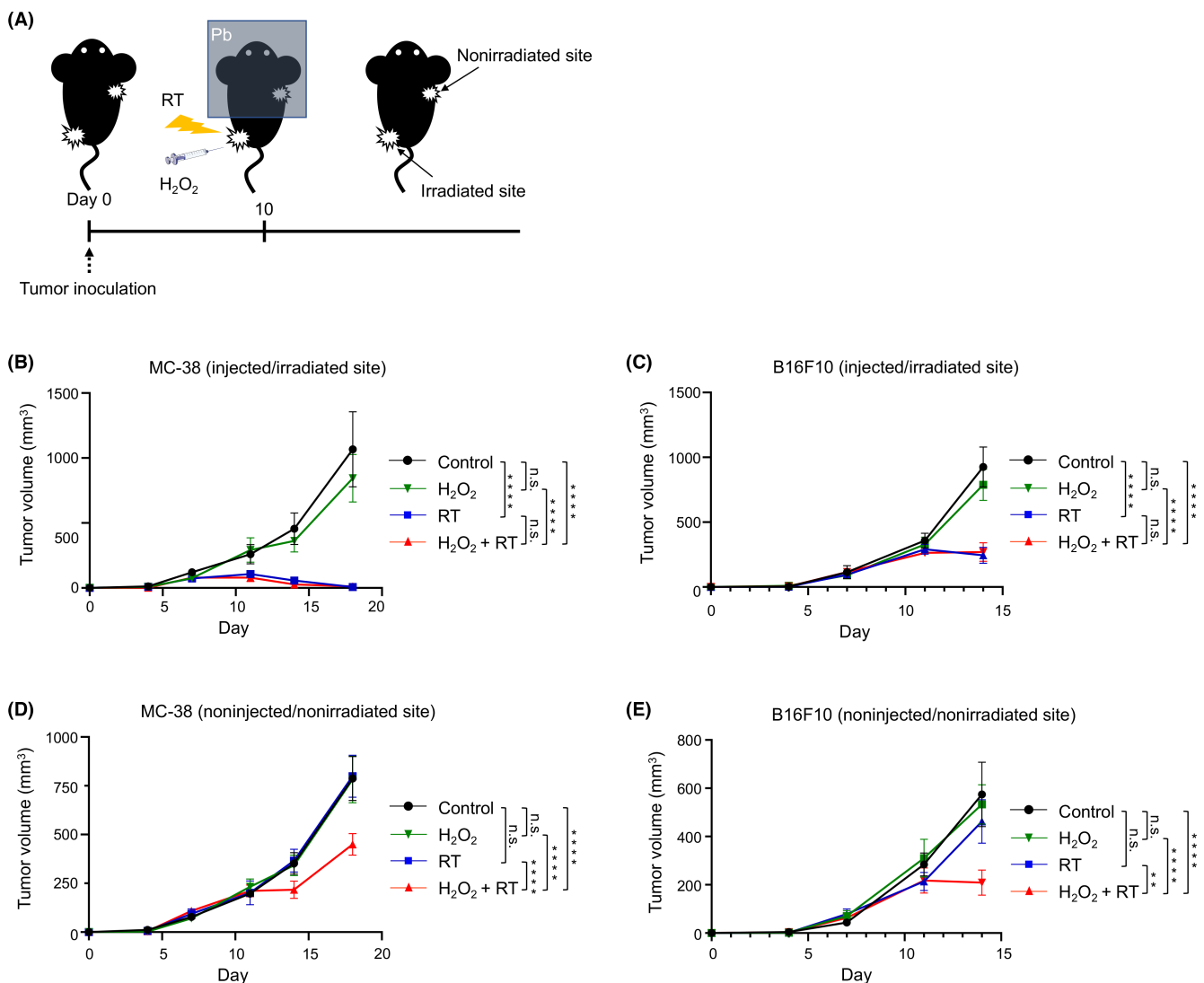


**FIGURE 1** In vivo efficacy of hydrogen peroxide/radiotherapy ( $H_2O_2$ /RT) combination treatment in wild-type immunocompetent mice. (A) Experimental schema. Cells were inoculated subcutaneously in the left hind limb and right back. Tumor volume was monitored every 3 days. When the tumor volume in the left hind limb reached approximately 100 mm<sup>3</sup> (before day 10),  $H_2O_2$  was administered intratumorally in the left hind limb. Within 30 min after dosing, 15-Gy single-dose irradiation was performed at the tumor sites. During irradiation, a custom fixation device was used to prevent irradiation to the tumors on the back. (B, C) Tumor growth at the injected/irradiated sites in wild-type immunocompetent mice ( $n=5$  per group). The data for MC-38 (B) and B16F10 (C) are shown. (D, E) Tumor growth in noninjected/nonirradiated sites of wild-type immunocompetent mice ( $n=5$  per group). The data for MC-38 (D) and B16F10 (E) are shown. All in vivo experiments were performed in duplicate and similar results were obtained. Two-way analysis of variance with Bonferroni's multiple comparisons test was used in (B)–(E) for statistical analyses. The means and SEMs are shown. \*\* $P < 0.01$ , \*\*\*\* $P < 0.0001$ ; n.s., not significant.

in the injected/irradiated sites was suppressed comparably in both the RT alone and H<sub>2</sub>O<sub>2</sub>/RT combination groups (Figure 1B,C). Tumor growth at the noninjected/nonirradiated site was also comparable among the control, H<sub>2</sub>O<sub>2</sub> alone, and RT alone groups; however, the suppression was significant in the H<sub>2</sub>O<sub>2</sub>/RT combination group (Figure 1D,E). These findings indicate that H<sub>2</sub>O<sub>2</sub> enhances the abscopal effect when combined with RT.

### 3.2 | The enhanced abscopal effect by H<sub>2</sub>O<sub>2</sub> administration is mediated through the immune system

We evaluated tumor growth using immunodeficient SCID (severe combined immunodeficiency) mice with the same experimental design to investigate the influence of the immune system (Figure 1A). Neither RT alone nor H<sub>2</sub>O<sub>2</sub>/RT combination treatment suppressed tumor growth at the noninjected/nonirradiated site, and there was no significant difference from the other groups (Figure 2A,B),

therefore the H<sub>2</sub>O<sub>2</sub>/RT combination treatment induces the abscopal effect via the immune system.

We evaluated DAMPs, which are released after cellular stresses such as cell death and damage, and could influence the abscopal effect.<sup>19,20</sup> HMGB1 is a multifunctional protein. In the nucleus, HMGB1 acts as a chromatin conformational change factor that converts the conformation of chromatin to an optimal state for transcription by replacing histone H1 and relaxing the nucleosome structure; it is widely recognized as one of the DAMPs.<sup>19–22</sup> HMGB1 in the supernatant of cultured MC-38 cells was significantly increased in the RT alone group, and the addition of H<sub>2</sub>O<sub>2</sub> further increased the release in a concentration-dependent manner (Figure 3A). Next, we analyzed the cell surface expression of calreticulin, a protein regulating intracellular Ca<sup>2+</sup> homeostasis and the Ca<sup>2+</sup> capacity of the endoplasmic reticulum, using flow cytometry.<sup>19,20</sup> Calreticulin on the cell surface activates antitumor immunity.<sup>23</sup> Calreticulin expression on the cell surface was significantly increased by H<sub>2</sub>O<sub>2</sub> alone in a concentration-dependent manner; this was further increased by the combination with RT (Figure 3B).

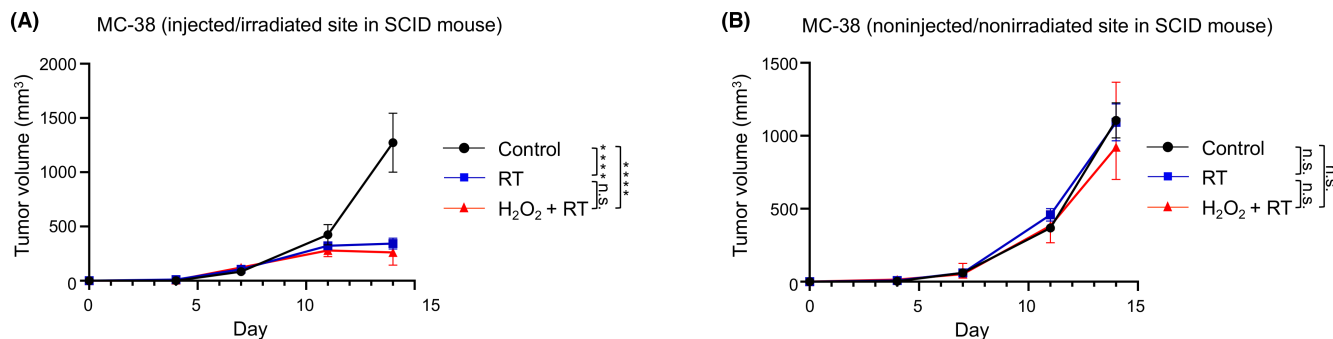


**FIGURE 2** In vivo efficacy of hydrogen peroxide/radiotherapy (H<sub>2</sub>O<sub>2</sub>/RT) combination treatment in immunodeficient SCID mice. In vivo experiments were performed as described in Figure 1A, using the MC-38 cell line and immunodeficient SCID mice (*n* = 5 per group). The data for the injected/irradiated (A) and noninjected/nonirradiated (B) sites are shown. All in vivo experiments were performed in duplicate and similar results were obtained. Two-way analysis of variance with Bonferroni's multiple comparisons test was used for statistical analysis. The means and SEMs are shown. \*\*\*\**P* < 0.0001; n.s., not significant.

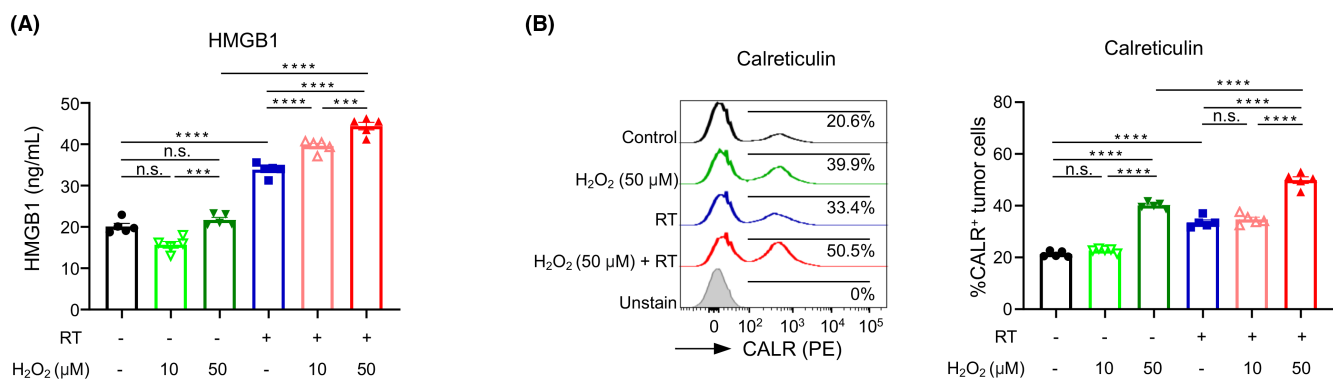


**FIGURE 3** DAMPs evaluated in vitro. MC-38 cells were treated with hydrogen peroxide (H<sub>2</sub>O<sub>2</sub>), radiotherapy (RT), or a combination of the two. Twenty-four hours later, the supernatants and cells were collected for HMGB1 and calreticulin assays, respectively. HMGB1 levels were measured using ELISA, and calreticulin expression on the cell surface was analyzed using flow cytometry. HMGB1 concentration (A) and calreticulin expression (B) are shown. In vitro experiments were performed in quintuplicate. One-way analysis of variance with Bonferroni's multiple comparisons test was used for statistical analysis. The means and SEMs are shown. \*\*\**P* < 0.001, \*\*\*\**P* < 0.0001; n.s., not significant; CALR, calreticulin; PE, phycoerythrin.

H<sub>2</sub>O<sub>2</sub>/RT combination treatment can therefore further activate antitumor immunity by releasing and exposing DAMPs compared to individual treatments.

### 3.3 | The H<sub>2</sub>O<sub>2</sub>/RT combination treatment activates antitumor immunity in the noninjected/nonirradiated site

DAMPs are recognized by pattern recognition receptors (PRRs) on dendritic cells (DCs), leading to the activation and maturation of DCs,<sup>19,20</sup> therefore we analyzed DCs in TDLNs. Flow cytometric

analysis of irradiated areas revealed a significant increase in the number of DCs (CD11c<sup>+</sup>I-A/I-E<sup>+</sup>) in the TDLNs from the H<sub>2</sub>O<sub>2</sub>/RT combination group compared to that in the control and RT alone groups (Figure 4A). Next, we evaluated DC maturation; CD80 and CD86 are the most common indicators of DC maturation.<sup>24</sup> The expressions of both CD80 and CD86 were significantly increased in the DCs in the H<sub>2</sub>O<sub>2</sub>/RT combination group compared to that in the other groups (Figure 4B,C). In addition, a significant increase in MHC class II expression in DCs was observed in the H<sub>2</sub>O<sub>2</sub>/RT combination group (Figure 4D).

We next investigated tumor-infiltrating lymphocytes (TILs) at the noninjected/nonirradiated sites using flow cytometry. We found a

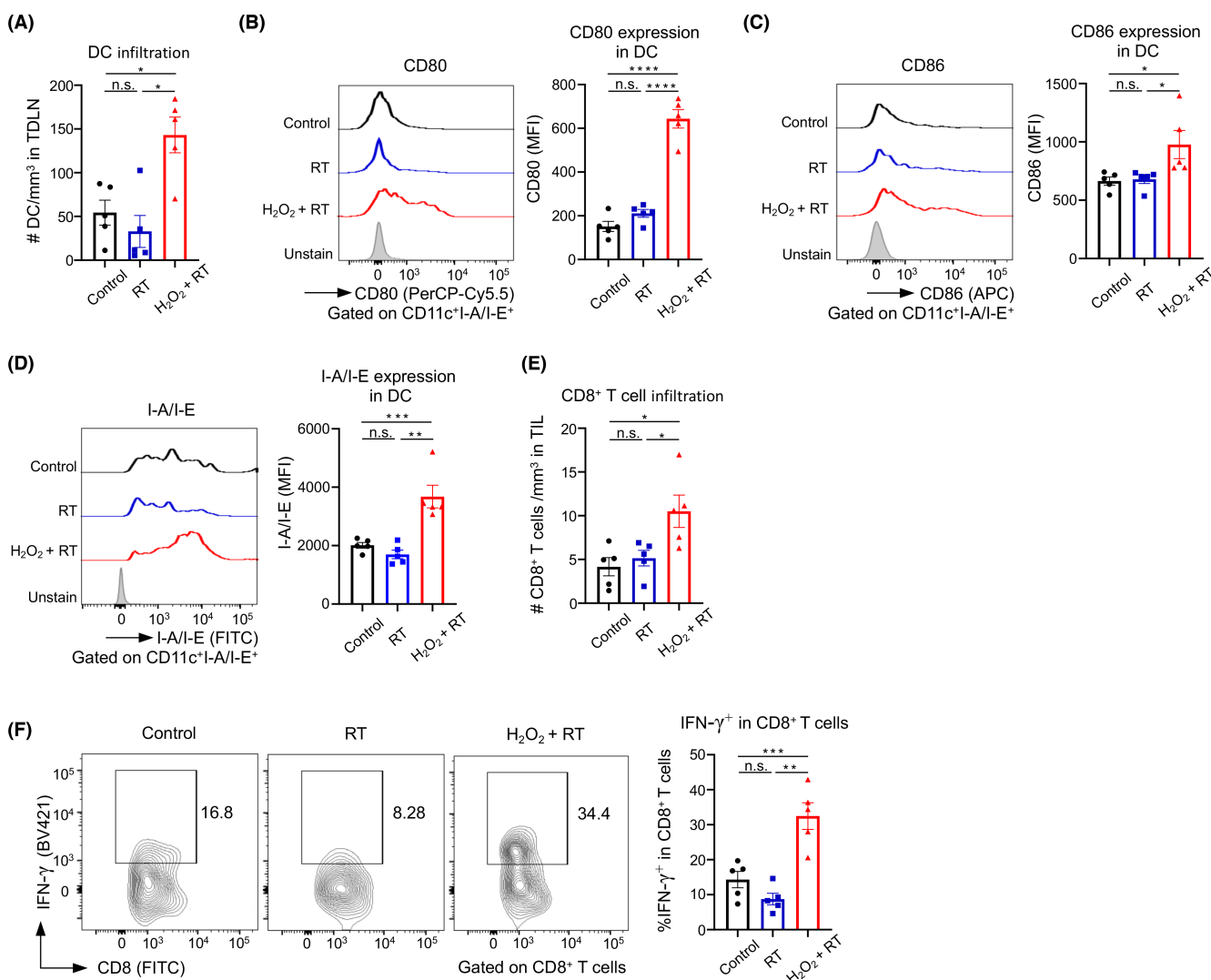


**FIGURE 4** Tumor-draining lymph node (TDLN) and tumor-infiltrating lymphocyte (TIL) analyses. In vivo experiments were performed as described in Figure 1A, using the MC-38 cell line and immunocompetent wild-type mice. TDLNs in the irradiated/injected areas and tumors in the noninjected/nonirradiated areas were harvested on day 14 for evaluation using flow cytometry ( $n = 5$  per group). (A) Number of dendritic cells (DCs) in TDLNs at the irradiated/injected areas. (B–D) CD80 (B), CD86 (C), and I-A/I-E (D) expression in DCs in TDLNs at the irradiated/injected areas. Representative flow cytometry staining (left) and summary (right) are shown. (E) The number of CD8<sup>+</sup> T cells in the noninjected/nonirradiated tumors. (F) The proportion of IFN-γ<sup>+</sup>CD8<sup>+</sup> T cells in noninjected/nonirradiated tumors. Representative flow cytometric staining (left) and summary (right) images are shown. One-way analysis of variance with Bonferroni's multiple comparisons test was used for statistical analysis. The means and SEMs are shown. \* $P < 0.05$ , \*\* $P < 0.01$ , \*\*\* $P < 0.001$ , \*\*\*\* $P < 0.0001$ ; n.s., not significant. H<sub>2</sub>O<sub>2</sub>, hydrogen peroxide; RT, radiotherapy.

significant increase in the number of CD8<sup>+</sup> T cells in tumors in the H<sub>2</sub>O<sub>2</sub>/RT combination group compared to that in the control or RT alone group (Figure 4E). In addition, the frequency of IFN-γ<sup>+</sup>CD8<sup>+</sup> T cells was significantly increased in the H<sub>2</sub>O<sub>2</sub>/RT combination group (Figure 4F). Altogether, the H<sub>2</sub>O<sub>2</sub>/RT combination treatment increased DC infiltration and maturation, leading to the abscopal effect via T-cell activation at the nonirradiated/noninjected sites.

### 3.4 | H<sub>2</sub>O<sub>2</sub>/RT combination with anti-PD-1 mAb shows additional tumor regression

Cancer immunotherapy has been used in clinical settings in recent years.<sup>25</sup> Cancer immunotherapy can activate antitumor immunity; combination treatment with PD-1 blockade and RT can further

increase antitumor immunity and is more likely to generate abscopal effects.<sup>26</sup> We therefore added anti-PD-1 mAb to the same model (Figure 5A); we found complete tumor regression in the injected/irradiated site (Figure 5B) and significant tumor regression in the noninjected/nonirradiated site (Figure 5C). These results indicate that the combination of H<sub>2</sub>O<sub>2</sub>, RT, and anti-PD-1 mAb is more likely to induce an abscopal effect.

## 4 | DISCUSSION

RT exhibits antitumor effects through DNA cleavage and free radical generation.<sup>1,2</sup> The presence of abundant oxygen increases free radical production because oxygen molecules are powerful oxidants. However, as the tumor grows, the tumor core becomes

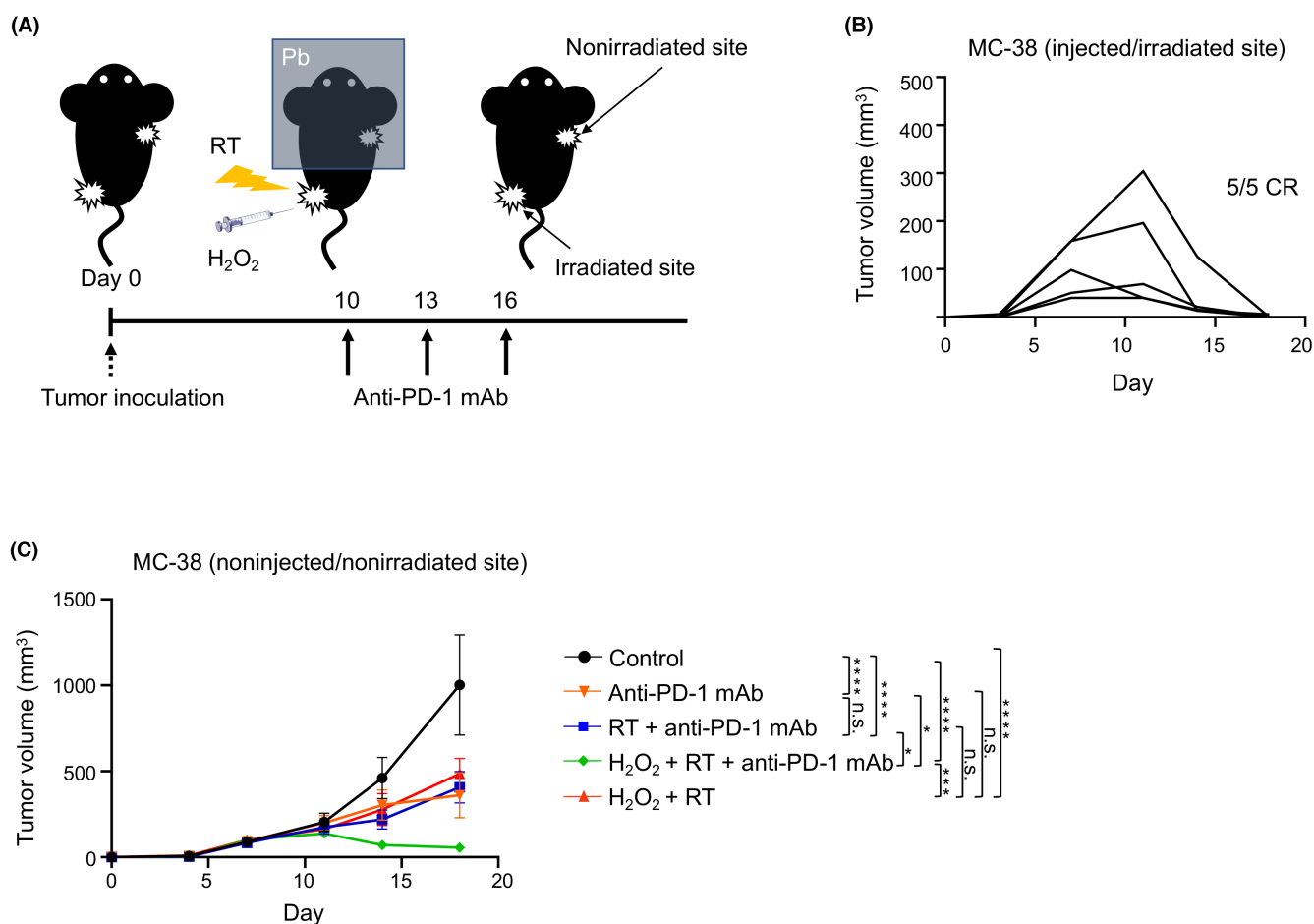


**FIGURE 5** In vivo efficacy of combination with hydrogen peroxide (H<sub>2</sub>O<sub>2</sub>), radiotherapy (RT), and anti-PD-1 mAb. (A) Experimental schema. Cells were inoculated subcutaneously in the left hind limb and right back. Tumor volume was monitored every 3 days. When the tumor volume in the left hind limb reached approximately 100 mm<sup>3</sup> (before day 10), H<sub>2</sub>O<sub>2</sub> was administered intratumorally in the left hind limb. Within 30 min after dosing, 15-Gy single-dose irradiation was administered to the same tumor. During irradiation, a homemade fixation device was used to prevent irradiation to the tumors on the back. Anti-PD-1 mAb (200 μg/mouse) or control mAb was administered intraperitoneally three times every 3 days after H<sub>2</sub>O<sub>2</sub> injection or irradiation. (B, C) Tumor growth in the injected/irradiated sites (B) and the noninjected/nonirradiated sites (C) of wild-type immunocompetent mice (*n* = 5 per group). The data of MC-38 are shown. CR, complete regression. All in vivo experiments were performed in duplicate and similar results were obtained. Two-way analysis of variance with Bonferroni's multiple comparisons test was used for statistical analysis. The means and SEMs are shown. \**P* < 0.05, \*\*\**P* < 0.001, \*\*\*\**P* < 0.0001; n.s., not significant.

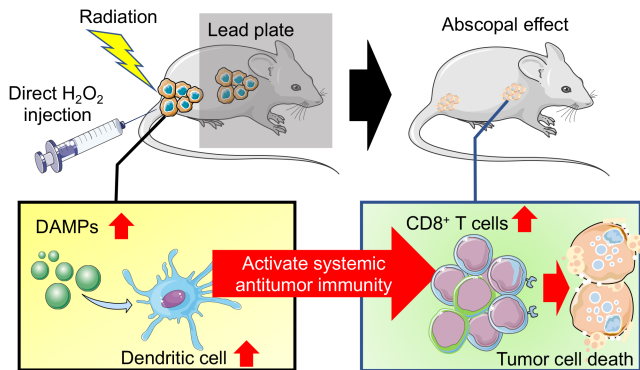


**FIGURE 6** Summary of the abscopal effect by hydrogen peroxide ( $\text{H}_2\text{O}_2$ )/radiotherapy (RT) combination treatment. Intratumoral administration of  $\text{H}_2\text{O}_2$  combined with RT increases the release of damage-associated molecular patterns (DAMPs), leading to dendritic cell infiltration and maturation. This results in the activation of antitumor immunity and the suppression of tumor growth in noninjected/nonirradiated tumors.

hypoxic; in addition, the tumor produces excess amounts of antioxidant enzymes to protect itself from reactive oxygen species, which makes local control of the tumor by RT difficult.<sup>3</sup> Ogawa et al. therefore developed a method to inject  $\text{H}_2\text{O}_2$  directly into the tumor.<sup>4</sup> Neutralizing with  $\text{H}_2\text{O}_2$ , an active oxygen, eliminates antioxidant enzymes such as peroxidase with the production of oxygen as the end product; this ameliorates hypoxia. In addition,  $\text{H}_2\text{O}_2$  itself causes DNA damage and induces cell death via apoptosis and necrosis<sup>27–30</sup>; exposure to  $\text{H}_2\text{O}_2$  may increase the expression of inflammatory cytokines.<sup>31,32</sup> KORTUC®, a mixture of  $\text{H}_2\text{O}_2$  and sodium hyaluronate, was developed for clinical applications in the UK and Japan.<sup>6,7</sup>

The abscopal effect is defined as the simultaneous regression of both the irradiated tumor and the tumor outside the irradiated area. This effect is seen relatively rarely in clinical settings.<sup>9–15</sup> In this study, we found that intratumoral injection of  $\text{H}_2\text{O}_2$  immediately followed by irradiation suppressed tumor growth in mouse models not only at the irradiated site, but also at the noninjected/nonirradiated site. There are various hypotheses explaining the abscopal effect; one hypothesis is that irradiation activates antitumor immunity, which kills distant tumor cells.<sup>16</sup> There is an increase in  $\text{CD8}^+$  T cells in TILs following chemoradiotherapy, partly due to radiation-induced reprogramming of the tumor microenvironment toward antitumor immune responses.<sup>33,34</sup> Radiation reportedly activates DCs in tumors<sup>35</sup>; a significant increase in mature DCs was observed in TDLNs in the mouse model used in this study. In addition, we found significant increases in  $\text{CD8}^+$  T-cell infiltration and  $\text{IFN-}\gamma$  production in  $\text{CD8}^+$  T cells of noninjected/nonirradiated tumors. In vitro experiments showed that HMGB1 release and calreticulin expression on the cell surface increased in the  $\text{H}_2\text{O}_2$ /RT combination treatment. These molecules are DAMPs that are recognized by PRR on DCs, leading to DC maturation,<sup>19,20</sup> therefore  $\text{H}_2\text{O}_2$ /RT combination treatment promotes DC maturation via increased DAMPs, leading to activated systemic antitumor immunity.

We irradiated mice with 15 Gy in one fraction. Although this dose is rarely used in clinical settings, hypofractionated radiotherapy has been reported to induce a strong abscopal effect.<sup>36</sup> In this present study, we used the same dose and fraction as those previously reported in the  $\text{H}_2\text{O}_2$  study,<sup>37</sup> resulting in an abscopal effect. However, the optimal dose and fraction for the abscopal effect are yet to be determined. Thus, the optimal irradiation method to induce the strongest abscopal effect should be determined in future research.

PD-1 blockade exerts its antitumor effect by activating T-cell immune responses, which may be more effective when combined with RT.<sup>35</sup> The combination of PD-1 blockade therapy and RT has been effective in several clinical trials. In addition, the administration of PD-1/PD-L1 inhibitors with local RT to the metastatic site in advanced lung cancer can improve the patient's prognosis.<sup>38,39</sup> We have shown that antitumor immunity can be activated by  $\text{H}_2\text{O}_2$  intratumoral injection combined with RT in mouse models; in addition, we evaluated PD-1 blockade to the same mouse model. The combination of  $\text{H}_2\text{O}_2$ /RT with anti-PD-1 mAb further suppressed tumor growth at noninjected/nonirradiated sites, therefore the combination of  $\text{H}_2\text{O}_2$ , RT, and anti-PD-1 mAb could provide additional therapeutic benefits, even against advanced cancers.

In summary,  $\text{H}_2\text{O}_2$ /RT combination treatment activates antitumor immunity and suppresses tumor growth in noninjected/nonirradiated sites as an abscopal effect (Figure 6). The addition of PD-1 blockade further increased the antitumor effects at noninjected/nonirradiated sites. These findings indicate the promising efficacy of the combination of  $\text{H}_2\text{O}_2$ , RT, and anti-PD-1 mAb, even against advanced cancers.

#### AUTHOR CONTRIBUTIONS

NK: Data curation, formal analysis, investigation, visualization, and writing—original draft. LZ: Data curation, formal analysis, investigation, and writing—review & editing. JN: Investigation and writing—review & editing. YO: Investigation and writing—review & editing. YU: Writing—review & editing. HD: Writing—review & editing. YF: Writing—review & editing. ID: Writing—review & editing. YT: Conceptualization, funding acquisition, methodology, project administration, resources, validation, and writing—review & editing.

#### ACKNOWLEDGMENTS

We thank Ms. R. Inukai, M. Iwado, Y. Nishimori, M. Konishi, and S. Nakada for their technical assistance.

#### FUNDING INFORMATION

This study was supported by KORTUC Inc. (Tokyo, Japan).

#### CONFLICT OF INTEREST STATEMENT

I.D. received a research grant from Momotaro Gene outside this study. Y.T. received a research grant from KORTUC Inc. related to this study, research grants from KOTAI Biotechnologies, Daiichi-Sankyo, Ono Pharmaceutical, and Bristol-Myers Squibb outside of this study, and personal fees from Ono Pharmaceutical, Bristol-Myers Squibb, AstraZeneca, Chugai Pharmaceutical, MSD, and Sonire outside of

this study. All other authors declare that they have no competing financial interests. Y.T. is an Editorial Board Member of *Cancer Science*.

## ETHICS STATEMENT

Approval of the research protocol by an Institutional Reviewer Board: N/A.

Informed Consent: N/A.

Registry and the Registration No. of the study/trial: N/A.

Animal Studies: All animal experiments were approved by the Animal Committee for Animal Experimentation of Okayama University. All experiments met the U.S. Public Health Service Policy on Human Care and Use of Laboratory Animals.

## ORCID

Yue Fang  <https://orcid.org/0000-0002-0557-2118>

Yosuke Togashi  <https://orcid.org/0000-0001-9910-0164>

## REFERENCES

- Citrin DE. Recent developments in radiotherapy. *N Engl J Med*. 2017;377:1065-1075.
- Wang H, Mu X, He H, Zhang XD. Cancer radiosensitizers. *Trends Pharmacol Sci*. 2018;39:24-48.
- Hall EJ, Giaccia AJ. *Radiobiology for the Radiologist*. Vol 7. 8th ed. Wolters Kluwer; 2019:597.
- Tokuhiro S, Ogawa Y, Tsuzuki K, et al. Development of a novel enzyme-targeting radiosensitizer (KORTUC) containing hydrogen peroxide for intratumoral injection for patients with low linear energy transfer-radioresistant neoplasms. *Oncol Lett*. 2010;1:1025-1028.
- Ogawa Y, Kubota K, Ue H, et al. Safety and effectiveness of a new enzyme-targeting radiosensitization treatment (KORTUC II) for intratumoral injection for low-LET radioresistant tumors. *Int J Oncol*. 2011;39:553-560.
- Ogawa Y, Kubota K, Aoyama N, et al. Non-surgical breast-conserving treatment (KORTUC-BCT) using a new radiosensitization method (KORTUC II) for patients with stage I or II breast cancer. *Cancers (Basel)*. 2015;7:2277-2289.
- Nimalasena S, Gothard L, Anbalagan S, et al. Intratumoral hydrogen peroxide with radiation therapy in locally advanced breast cancer: results from a phase 1 clinical trial. *Int J Radiat Oncol Biol Phys*. 2020;108:1019-1029.
- Mole RH. Whole body irradiation; radiobiology or medicine? *Br J Radiol*. 1953;26:234-241.
- Golden EB, Chhabra A, Chachoua A, et al. Local radiotherapy and granulocyte-macrophage colony-stimulating factor to generate abscopal responses in patients with metastatic solid tumours: a proof-of-principle trial. *Lancet Oncol*. 2015;16:795-803.
- Bramhall RJ, Mahady K, Peach AH. Spontaneous regression of metastatic melanoma—clinical evidence of the abscopal effect. *Eur J Surg Oncol*. 2014;40:34-41.
- Postow MA, Callahan MK, Barker CA, et al. Immunologic correlates of the abscopal effect in a patient with melanoma. *N Engl J Med*. 2012;366:925-931.
- Ohba K, Omagari K, Nakamura T, et al. Abscopal regression of hepatocellular carcinoma after radiotherapy for bone metastasis. *Gut*. 1998;43:575-577.
- Wersall PJ, Blomgren H, Pisa P, Lax I, Kalkner KM, Svedman C. Regression of non-irradiated metastases after extracranial stereotactic radiotherapy in metastatic renal cell carcinoma. *Acta Oncol*. 2006;45:493-497.
- Cong Y, Shen G, Wu S, Hao R. Abscopal regression following SABR for non-small-cell-lung cancer: a case report. *Cancer Biol Ther*. 2017;18:1-3.
- Siva S, Callahan J, MacManus MP, Martin O, Hicks RJ, Ball DL. Abscopal effects after conventional and stereotactic lung irradiation of non-small-cell lung cancer. *J Thorac Oncol*. 2013;8:e71-e72.
- Rodríguez-Ruiz ME, Vanpouille-Box C, Melero I, Formenti SC, Demaria S. Immunological mechanisms responsible for radiation-induced abscopal effect. *Trends Immunol*. 2018;39:644-655.
- Nagasaki J, Inozume T, Sax N, et al. PD-1 blockade therapy promotes infiltration of tumor-attacking exhausted T cell clonotypes. *Cell Rep*. 2022;38:110331.
- Kawashima S, Inozume T, Kawazu M, et al. TIGIT/CD155 axis mediates resistance to immunotherapy in patients with melanoma with the inflamed tumor microenvironment. *J Immunother Cancer*. 2021;9:9.
- Galluzzi L, Vitale I, Warren S, et al. Consensus guidelines for the definition, detection and interpretation of immunogenic cell death. *J Immunother Cancer*. 2020;8:8.
- Krysko DV, Garg AD, Kaczmarek A, Krysko O, Agostinis P, Vandenabeele P. Immunogenic cell death and DAMPs in cancer therapy. *Nat Rev Cancer*. 2012;12:860-875.
- Andersson U, Tracey KJ. HMGB1 is a therapeutic target for sterile inflammation and infection. *Annu Rev Immunol*. 2011;29:139-162.
- Yang H, Antoine DJ, Andersson U, Tracey KJ. The many faces of HMGB1: molecular structure-functional activity in inflammation, apoptosis, and chemotaxis. *J Leukoc Biol*. 2013;93:865-873.
- Obeid M, Tesniere A, Ghiringhelli F, et al. Calreticulin exposure dictates the immunogenicity of cancer cell death. *Nat Med*. 2007;13:54-61.
- Sharpe AH, Freeman GJ. The B7-CD28 superfamily. *Nat Rev Immunol*. 2002;2:116-126.
- Reck M, Rodríguez-Abreu D, Robinson AG, et al. Pembrolizumab versus chemotherapy for PD-L1-positive non-small-cell lung cancer. *N Engl J Med*. 2016;375:1823-1833.
- Zhang Z, Liu X, Chen D, Yu J. Radiotherapy combined with immunotherapy: the dawn of cancer treatment. *Signal Transduct Target Ther*. 2022;7:258.
- Meneghini R. Iron homeostasis, oxidative stress, and DNA damage. *Free Radic Biol Med*. 1997;23:783-792.
- Imlay JA, Chin SM, Linn S. Toxic DNA damage by hydrogen peroxide through the Fenton reaction in vivo and in vitro. *Science*. 1988;240:640-642.
- Zhao M, Antunes F, Eaton JW, Brunk UT. Lysosomal enzymes promote mitochondrial oxidant production, cytochrome c release and apoptosis. *Eur J Biochem*. 2003;270:3778-3786.
- Kariya S, Sawada K, Kobayashi T, et al. Combination treatment of hydrogen peroxide and X-rays induces apoptosis in human prostate cancer PC-3 cells. *Int J Radiat Oncol Biol Phys*. 2009;75:449-454.
- Di Marzo N, Chisci E, Giovannoni R. The role of hydrogen peroxide in redox-dependent signaling: homeostatic and pathological responses in mammalian cells. *Cell*. 2018;7:7.
- Obata F, Hoshino A, Toyama A. Hydrogen peroxide increases interleukin-12 p40/p70 molecular ratio and induces Th2-predominant responses in mice. *Scand J Immunol*. 2006;63:125-130.
- Fujimoto D, Uehara K, Sato Y, et al. Alteration of PD-L1 expression and its prognostic impact after concurrent chemoradiation therapy in non-small cell lung cancer patients. *Sci Rep*. 2017;7:11373.
- Choe EA, Cha YJ, Kim JH, et al. Dynamic changes in PD-L1 expression and CD8(+) T cell infiltration in non-small cell lung cancer following chemoradiation therapy. *Lung Cancer*. 2019;136:30-36.
- Weichselbaum RR, Liang H, Deng L, Fu YX. Radiotherapy and immunotherapy: a beneficial liaison? *Nat Rev Clin Oncol*. 2017;14:365-379.



36. Liu Y, Dong Y, Kong L, Shi F, Zhu H, Yu J. Abscopal effect of radiotherapy combined with immune checkpoint inhibitors. *J Hematol Oncol*. 2018;11:104.
37. Akima R, Ogawa Y, Morita-Tokuhiro S, et al. New enzyme-targeting radiosensitizer (KORTUC) containing hydrogen peroxide & sodium hyaluronate for intra-tumoral injection using mice transplanted with SCC VII tumor. *Int J Cancer Clin Res*. 2016;3:3.
38. Antonia SJ, Villegas A, Daniel D, et al. Durvalumab after chemoradiotherapy in stage III non-small-cell lung cancer. *N Engl J Med*. 2017;377:1919-1929.
39. Theelen W, Chen D, Verma V, et al. Pembrolizumab with or without radiotherapy for metastatic non-small-cell lung cancer: a pooled analysis of two randomised trials. *Lancet Respir Med*. 2021;9:467-475.

## SUPPORTING INFORMATION

Additional supporting information can be found online in the Supporting Information section at the end of this article.

**How to cite this article:** Kemmotsu N, Zhu L, Nagasaki J, et al. Combination therapy with hydrogen peroxide and irradiation promotes an abscopal effect in mouse models. *Cancer Sci*. 2023;00:1-9. doi:[10.1111/cas.15911](https://doi.org/10.1111/cas.15911)